

**HEMATITE COATINGS MATCH TES SPECTRA OF SINUS MERIDIANI, MARS.** L. E. Kirkland<sup>1</sup>, K. C. Herr<sup>2</sup>, P. M. Adams<sup>2</sup>, J. W. Salisbury<sup>3</sup>; <sup>1</sup>Lunar and Planetary Institute, Houston, kirkland@lpi.usra.edu; <sup>2</sup>Aerospace Corp., kenneth.c.herr@aero.org, paul.m.adams@aero.org; <sup>3</sup>Johns Hopkins, *retired*, salisbury@worldnet.att.net.

**Introduction.** Lane et al. [1] and Christensen et al. [2] conclude that the 1996 Global Surveyor Thermal Emission Spectrometer (TES,  $\sim 1700\text{--}200\text{ cm}^{-1}$ ) spectra of regions in Sinus Meridiani match only coarsely particulate hematite.

Here we show spectra of hematite coatings that match the TES signatures. The coating option is important because (1) hematite coatings can require little water to form, which may significantly change current interpretations and explain the apparent absence of other alteration minerals; and (2) one 2003 rover is planned for this site, so researchers need to prepare for possible measurement of hematite coatings by the rover instruments. This includes adding coating signatures to interpretation libraries and addressing measurement issues related to a hematite coating.

**Spectral contrast.** Hematite has three absorption bands centered near 18, 23, and 33  $\mu\text{m}$ . These strong bands are called “reststrahlen bands.” When reststrahlen bands are observed as troughs with good spectral contrast, that indicates the presence of smooth-surfaced material in one of two broad forms: (1) closely packed or cemented fine particles (e.g., a coating or duricrust); (2) large particles.

There are two broad options because material can scatter light through two processes: surface and volume scattering [3]. A strong band is produced by high reflectance from the surface (surface scattering) when high opacity within the band gives it a mirror-like property. This produces reflectance peaks called “reststrahlen bands.” In emission, the surface reflects radiance inward at reststrahlen bands, causing an emissivity trough (e.g. Fig. 1 “solid surface”) [4].

When unconsolidated particles are small enough for light to survive passage through the grain, volume absorption (volume scattering) occurs [5]. When volume scattering dominates, the reststrahlen bands appear as emission peaks (Fig. 1, lower trace).

**Coarse vs. coating.** Volume scattering dominates for optically thin materials, and most materials become optically thin at small particle sizes. This causes very small hematite particles to have very low spectral contrast (e.g., Fig. 1 upper trace), which is contrary to the TES observations. This reasoning has been used to rule out the presence of finely particulate hematite as the source of the observed TES signatures.

However, when optically thin particles are close ( $\sim$ wavelength) together, they scatter coherently, and behave as if they were larger particles [5]. This occurs for cemented, fine particles (e.g. as may occur in duricrust and desert varnish). Differences in the

relative contribution from surface and volume scattering will affect the band depths, shapes, and widths.

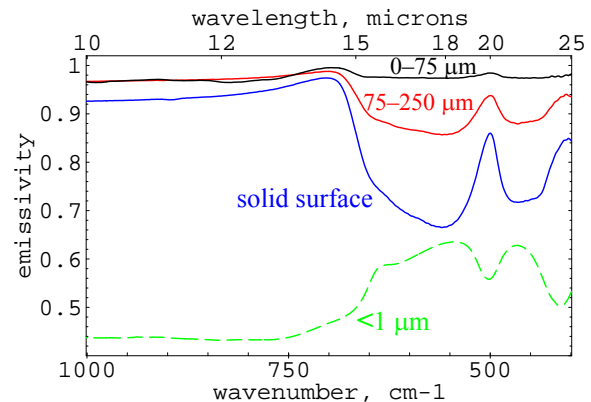


**Fig. 1. Surface vs. volume scattering.** Surface scattering dominates the “solid surface” spectrum, causing reststrahlen emissivity troughs. Volume scattering dominates the optically thin,  $<1\ \mu\text{m}$  particles, causing emissivity peaks. Volume scattering contributes to the spectral contrast decrease in the 75–250  $\mu\text{m}$  and 0–75  $\mu\text{m}$  samples. Sample “hematite.1”, from [6], shown in 1 - biconical reflectance (upper traces) or 1- transmission (lower trace).

**Match to Mars data.** Fig. 2 shows spectra of coarsely particulate hematite [7], hematite coatings, and a TES spectrum from Sinus Meridiani. The Fig. 2 TES spectrum has an atmospheric compensation applied using the methods in [8]. We use only data measured by detector 5 to decrease instrumental effects. The hematite coatings were characterized using X-ray Diffraction (XRD) and the spectral signature itself. The coatings are smooth, lustrous, and usually black. The visible spectrum of example black coatings matched the spectrum of coarse hematite.

Fig. 3 shows a Scanning Electron Microscope (SEM) cross-section of an example hematite coating. The spectra show that the coating is optically thick over the 18–50  $\mu\text{m}$  range. Some samples are slightly translucent in the  $\sim 7\text{--}13\ \mu\text{m}$  range, which is evident when the substrate signature can also be seen (Fig. 4).

**Discussion.** Hematite coatings are a good match to the TES data, and may in fact match better than coarsely particulate hematite in two important areas: (1) the coarsely particulate hematite has a wider 18  $\mu\text{m}$  band than the TES signatures [9]; (2) the coarsely particulate hematite has mismatches in the band centers (Fig. 2 dashed lines).

## INFRARED SPECTRA OF HEMATITE: L. E. Kirkland et al.

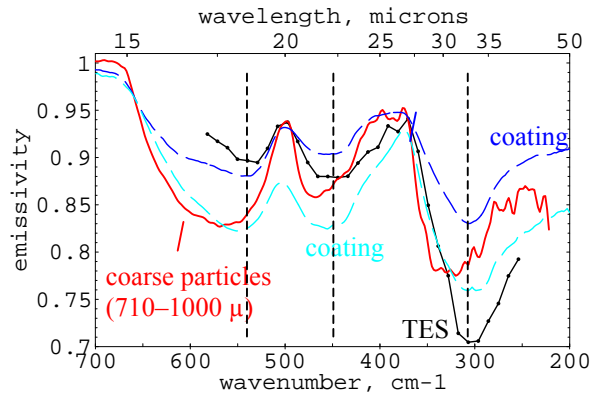


**Fig. 2. Hematite: Coatings, Coarse particles, TES.** The two dashed traces show hematite coating signatures. The solid trace shows coarsely particulate hematite [7]. The TES spectrum is of Sinus Meridiani, scaled to plot with a similar spectral contrast for comparison of the band shapes. The dashed vertical line illustrates the improved match of the coating to the observed band centers. (Footnote has sample details).

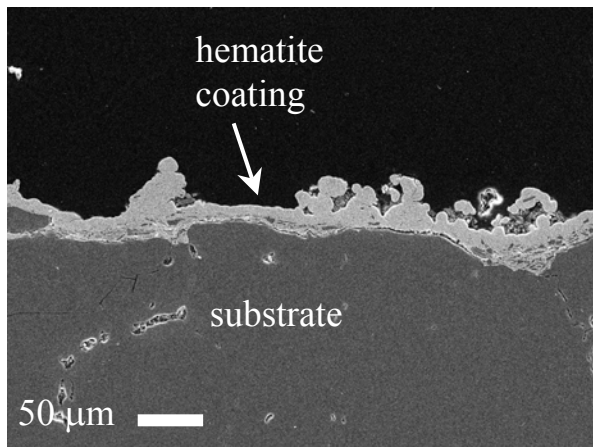


**Figure 3: Hematite coating.** SEM cross-section image of a hematite film that formed on a quartz substrate. SEM images measured of different areas of the sample show that the coating is  $\sim 10\text{--}40\ \mu\text{m}$  thick. This sample (bhm3) was from near Bunker Hill Mine, eastern Inyo Mountains, Saline Valley, Inyo County, California.

There is debate about whether the very small feature near  $26\ \mu\text{m}$  is present in the TES spectra (e.g., Fig. 2). Some of the coatings have this feature and others do not, and there are other small variations. Causes of the variations include scattering and preferred crystal orientation effects, as well as contaminants. These effects have received little attention, and should be studied.

Hematite has high opacity at these wavelengths, so a very thin coating (Fig. 3) can both behave spectrally as large particles and also mask the substrate (Figs. 2 and 4). If the coating is sufficiently thin, the substrate

signature may be seen (Fig. 4). However, the signature may appear distorted because the coating opacity varies with wavelength. In our examples, the substrate is quartz, but on Mars basalt is more likely.

A hematite coating matches the TES signatures. Other cemented materials should also be studied, e.g., ferricrete [10].

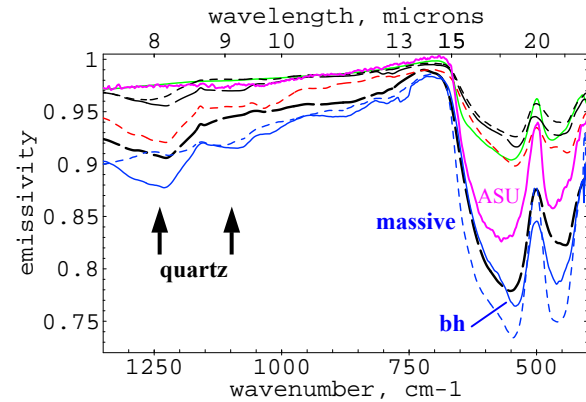


**Figure 4: Hematite-rich coatings and massive hematite.** Black traces are spectra of black coatings; the red trace is a red coating (sample bhm5); the green trace is massive martite, all measured in biconical reflectance and converted to approximate emissivity using one - reflectance. The blue dashed trace ("massive") is of massive hematite, and the blue solid trace ("bh") is of a black coating (sample bhm3), measured in hemispherical reflectance and converted to emissivity using one - reflectance. Quartz causes the weak features in the  $\sim 8\text{--}9\ \mu\text{m}$  region, and quartz or clay may contribute to the sharper band near "bh". The purple trace ("ASU") is of  $710\text{--}1000\ \mu\text{m}$  hematite particles from [7].

**Fig. 2 sample details:** Coatings: blue="bhm3\_blk\_a"; blue-green="bhm4\_blk\_b", in approximate emissivity using 1-biconical reflectance. TES signature: average of 11 TES spectra (ICK 643888002 to -024), in apparent emissivity, with an atmospheric compensation applied using the methods in [8], and scaled using  $(3 \times x) - 2$ . TES lab spectrum: "bur2600" [7], with a 3-point boxcar smoothing to increase the signal-to-noise ratio, measured in emission, then converted to apparent emissivity with respect to  $690.4\ \text{cm}^{-1}$ .

**References:** [1] Lane M. et al. (1999) *LPSC abs. 1469*. [2] Christensen P. et al. (2000) *JGR 105*, 9632. [3] Vincent R.K. and Hunt G. R. (1968) *Appl. Opt.* 7, 53. [4] Planck M. (1914) *The Theory of Heat Radiation*. [5] Salisbury J. and Wald A. (1992) *Icarus 96*, 121. [6] Salisbury J.W. et al. (1991) *Infrared (2.1–25 μm) Spectra of Minerals*. [7] Christensen P. et al. (2000) *JGR 105*, 9735. [8] Kirkland L. E. et al. (2002), First Use of an Airborne Thermal Infrared Hyperspectral Scanner for Compositional Mapping, *Remote Sens. Environ.* 80, 447, [www.lpi.usra.edu/science/kirkland](http://www.lpi.usra.edu/science/kirkland). [9] Kirkland, L. E. et al. (1999) *LPSC XXX*, abs. 1693; Kirkland, L. E. et al. (2001) *Eos Trans. AGU*, 82(20), abs. S242. [10] Kirkland, L. E. et al. (2002), *LPSC XXXIII*, abs. 1218.